INVESTIGATION OF BOUNDARY LAYER TRANSITION FOR SMALL REYNOLDS NUMBERS IN FREE FLIGHT AND WIND TUNNEL EXPERIMENTS

Bernhard Kobiela
Institut für Thermodynamik der Luft- und Raumfahrt
Universität Stuttgart

Abstract

In aerodynamic engineering the e^n transition criterion is widely used to calculate the beginning of transition in a two-dimensional boundary layer. It is assumed that the transition starts when the Tollmien-Schlichting-waves have reached $e^{n_{crit}}$ -times the size of their initial value in the instability-point. The critical amplification factor n_{crit} is measured for Reynolds numbers below 600,000 both in the laminar wind tunnel of the "Institut für Aerodynamik und Gasdynamik" at the "Universität Stuttgart" and for the first time in free flight tests in calm air. A method is developed to adequately determine the pressure distribution of the test profile without direct measurement and to aquire the transition position quantitatively and in a repeatable way. A symmetric test profile with no laminar separation at an angle of attack of 0° is used which shows minimal interdependencies between viscous and non-viscous areas and allows a sufficiently precise calculation of the airflow around the profile. Because of the symmetry an angle of attack of 0° can easily be detected. With the test airfoil vertically attached to a model airplane the lift coefficient c_L of the test profile is independent of the flight velocity, i.e. $c_L = 0$ can be realised for all flight velocities. Transition position is measured by two symmetrically arranged Preston tubes. The related n-factor is determined by means of an incompressible Orr-Sommerfeld-solver. The determined averaged critical amplification factor for Reynolds numbers between 300,000 and 600,000 is $n_{crit} = 12.6$ with a deviation of $\Delta n_{crit} = 0.1$ in the wind tunnel and $\Delta n_{crit} = 0.6$ in free flight.

...

Nomenclature

Symbols

A	$[\frac{m}{s}]$	Interference amplitude
A_0	$[\frac{m}{s}]$	Interference amplitude in the instability point
c_L	[-]	Lift coefficient
c_p	[-]	Pressure coefficient
d	[m]	Eddy diameter
f	[Hz]	Frequency
H_{12}	[-]	Form parameter of the boundary layer
n	[-]	Amplification factor
n_{crit}	[-]	Amplification factor at the beginning of transition
q	[bar]	Dynamic pressure
Re	[-]	Reynolds number
s	[m]	Profile contour length
Tu	[-]	Turbulence level
u	$[\frac{m}{s}]$	Velocity
α	[°]	Angle of attack

Indices

∞	Free stream
$Preston$	Preston tube

Abbreviations

TS-frequency	Frequency of a TS-wave
TS-wave	Tollmien-Schlichting-wave

1 Introduction

The position of the laminar-turbulent boundary layer transition strongly influences the air flow around an object. In technical engineering the beginning of the boundary layer transition is calculated by use of suitable transition criteria. The $\mathrm{e^n}$-criterion is frequently used. It is assumed that the transition starts when the Tollmien-Schlichting-waves (TS-waves) have reached $e^{n_{crit}}$ -times the size of their initial value. The n-factor n_{crit} needs to be experimentally determined for given flow conditions as the initial value can depend on the free stream turbulence. The transition position can be determined in a wind tunnel. Nevertheless the question whether the results are also valid for flights in free atmosphere remains unanswered as turbulences may differ between the wind tunnel and free flight.

Transition measurements for Reynolds numbers greater than 1,000,000, which are common in general aviation aircrafts, are available by Kroneberger [12] and Miley, Horstman and Quast [17], [7], [8]. Kroneberger developed a multisensor hot film array and investigated the amplification and dispersion of TS-waves on top of a "glove" adjusted to the airfoil of the power glider "Grob G109 Brq' in free flight and in a wind tunnel. The author determined the critical amplification factor as $n_{crit} = 9$. Miley, Horstman and Quast analysed the TS development in laminar boundary layers by means of hot wire anemometers and the critical amplification factor on the airfoil of a single engined, four seated aircraft by means of infrared thermal images. Measurements were taken in the German-Dutch wind tunnel (DNW) and in free flight. The determined n_{crit}-factors were between 12 and 15.

For smaller Reynolds numbers comparable measurements are lacking, although precise knowledge of the n_{crit}-factor is even more essential as the TS-wave amplification is much slower. Thus a given uncertainty in n_{crit} results in considerable greater deviations of the calculated transition position. In the presented experiments the critical amplification factor n_{crit} of the interference amplitudes of the TS-waves up to the start of transition is determined for Reynolds numbers below 600,000 in the laminar wind tunnel of the "Institut für Aerodynamik und Gasdynamik IAG" at the "Universität Stuttgart" and in free flight. To this end start of transition is measured on a suitable profile. The TS amplification up to that position is calculated according to the linear stability theory for laminar boundary layers. Lerch [13] measured n_{crit} for Reynolds numbers below 1,000,000 using the measurement and analysis methods developed in the work reported here. Lerch attached the same airfoil as used in the present work to the glider Duo Discus T. The author took measurements near Basel in free flight above 2,000 metres altitude in calm air, above an inversion layer. The determined n_{crit} of 12.8, is almost identical to the present results, see Kobiela et al. [10], [11].

2 Underlying principles

2.1 Flow phenomena

The boundary layer is divided into several areas starting in the stagnation point, following the profile contour until reaching the trailing edge. From the stagnation point up to the instability point the flow is laminar and stable. Interferences in that area are damped down. Behind the instability point an instable laminar flow follows until transition start. In that area TS-waves are amplified until their amplitudes reach a critical size and turbulent transition starts. According to Würz the critical point ist reached when the interference velocity is about 10% of the mean velocity [20]. The amplification can initially be described by means of the linear stability theory. When the TS-waves reach a critical size of about 1% of the mean velocity they show non-linear amplification, i.e. modified amplification rates. Non-linear amplification is a current research topic which could not be considered here.

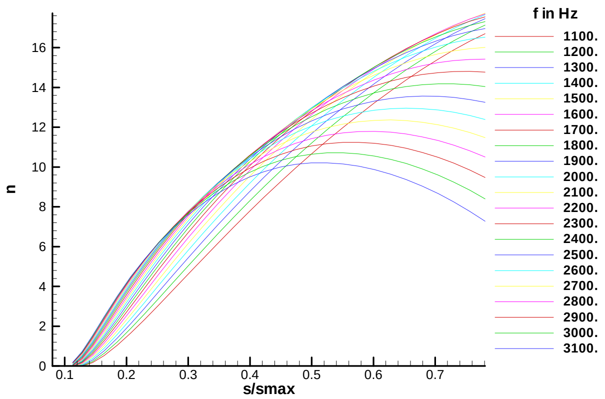

FIG. 1: Interference development at the measurement profile at $Re = 400,000$ according to the linear stability theory

According to the linear stability theory a narrow frequency range of TS-waves is amplified, which shifts towards higher frequencies with increasing free stream Reynolds numbers. Figure 1 displays the course of the TS amplitude for the straightly moving TS-waves of differing frequencies against the dimensionless contour length of the profile $\frac{s}{s_{max}}$ for a constant Reynolds number of incoming flow. At the axis of ordinates the amplification factor $n = \ln \frac{A}{A_0}$ of a TS amplitude A compared to the TS amplitude in the instability point A_0 is displayed. This amplification factor can be computed using the linear stability theory. The interference in the instability point A_0 is unknown. To increase clearness of the figure, the interference is logarithmically displayed and the amplification factor is named n instead of $\frac{A}{A_0}$.

According to the theory underlying the e^n-criterion the laminar-turbulent transition starts when the largest amplitude of a single TS-wave reaches a critical size. The absolute size of the interference is thus dependent on the amplification factor n, which results from the pressure distribution, the free stream Reynolds number and the initial TS amplitude in the instability point A_0. If the initial interference is sufficiently stable, a critical amplification factor n_{crit} can be determined, which is reached at the start of transition.

Interferences impinging on the profile with TS-frequency can couple to the boundary layer to a certain extent. That process is called receptivity [18]. It was investigated in the laminar wind tunnel of the IAG by

Herr [6]. According to Bertolotti [1] the direct interference coupling is circumstantial. The author considers indirect interference coupling to be more influencial. It is caused by big vortices with a low frequency that deform the boundary layer.
In the transition area the spectrum of TS frequencies broadens in bandwidth and the TS amplitudes increase considerably. The mean velocity profile of the boundary layer transforms. In particular the velocity close to the wall and the velocity gradient at the wall increase, which leads to an increase in wall shear stress. When the transformation of the velocity profile is completed, the transition area ends and turbulent flow is given.
In the present work the transition start is defined to take place at the point where the timely averaged velocity profile of the boundary layer starts to transform due to turbulences.

2.2 Calculation of the TS amplification

The calculation of TS amplification in the laminar boundary layer takes place in several steps. The pressure distribution on the profile contour is calculated using XFoil [4], which is a profile calculation programme working with a second order panel method and a coupled, integral boundary layer calculation. The flow transition is fixed to a point downstream of the expected position.
The velocity profiles are calculated on the basis of the determined pressure distribution by means of a finite difference programme [2]. A direct, incompressible Orr-Sommerfeld-solver [3] was used for the following stability calculation. That solver calculates the course of the amplification factor $n = \ln(\frac{A}{A_0})$ of the TS-waves amplitudes on the profile contour for each frequency seperately. In the calculation an incompressible flow is assumed. The slip angle of the calculated TS-waves is selectable. According to the Squire-theorem [15] the straightly moving wave is most amplified in the considered case and thus firstly reaches the critical size for flow transition. Therefore the stability calculation was limited to that wave. An exemplary result of the calculation can be seen in figure 1.

3 Measurement technique

Measurements in free athmosphere were done with the model airplane shown in figure 2. The requirements for the measurement, i.e. attached flow around the profile and a precise knowledge of the angle of attack as well as the pressure distribution, can be met with an adequate symmetrical profile and an angle of attack of $\alpha = 0\,°$. With symmetrical incoming flow the pressure difference between the profile sites vanishes and the transition positions are equal, thus the angle of attack can be easily checked. A further advantage is that no flow around the wing tip of the airfoil occurs. Thus three dimensional effects hardly falsify the mea-

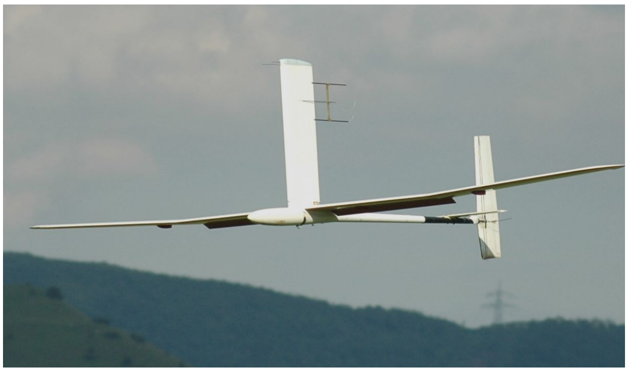

FIG. 2: The measurement airplane in approach for a landing

surement results as an angle of attack of $\alpha = 0\,°$ can be maintained over a wide range of velocities without interfering lifting forces.
The profile GW98109 (Graf [5]) is used as measurement profile. The profile is designed to possese maximal TS amplification at maximal distances, because the TS amplifications are very low for the investigated low Reynolds numbers and long unstable laminar sections result. This is achieved by long pressure risings, which are physically close to laminar seperation. From 20 % to 90 % of the profile depth the form parameter H_{12} is 3.3 if no laminar-turbulent transition takes places before. Assuming Falkner-Skan boundary layer profiles, laminar flow seperation occurs at $H_{12} = 4$.
Beginning at 90 % of the profile depth the profile is closed by a pressure rise which can only be overcome by turbulent flow. If that occurs symmetrically at too low Reynolds numbers the minimal threshold of the measurable range of Reynolds numbers is reached.
Problems arise if the measurement airfoil shows variations of the angle of attack, which are unavoidable on an airplane. On the pressure side the transition position shifts towards the trailing edge. If for low Reynolds numbers the laminar-turbulent transition area now reaches the closure pressure rise a separation bubble emerges at 90% of the profile depth, which not necessarily closes on top of the profile. That separation somewhat shifts the Kutta-condition away from the trailing edge towards the pressure side of the profile and thus increases the effective camber of the profile. According to calculations with XFoil this leads to a up to ten times overreaching lift gradient $\frac{\partial C_L}{\partial \alpha}$ around the zero position. A turbulator attached to 80 % of the profile depth helps reducing that problem, although not avoiding it. The profile is shown in figure 3. It can be seen that the calculated pressure distribution closely matches the measurements in the model wind tunnel of the Institut für Aerodynamik und Gasdynamik [14].
The measurement airfoil has a depth of 220 mm and a height of 600 mm. The exact dimensions are shown in figure 4. The airfoil is build in a negative mould in a glass-fibre reinforced plastic sandwich construction.
The measurement airfoil is perpendicularly attached

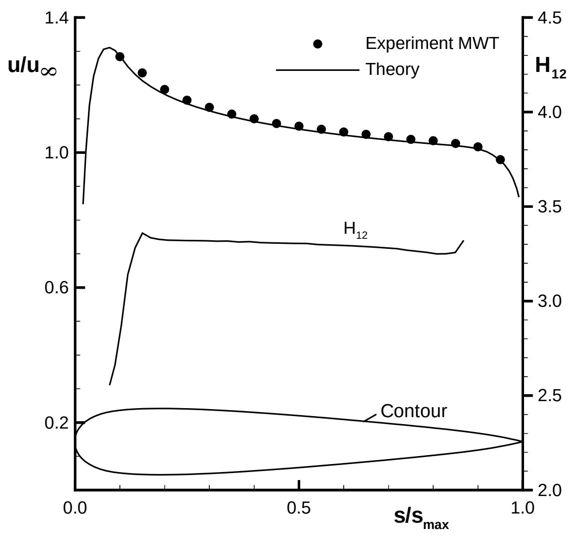

FIG. 3: Pressure distribution and course of the form parameter at the profile GW98109, $Re = 250,000$, from Lutz et al. [14]

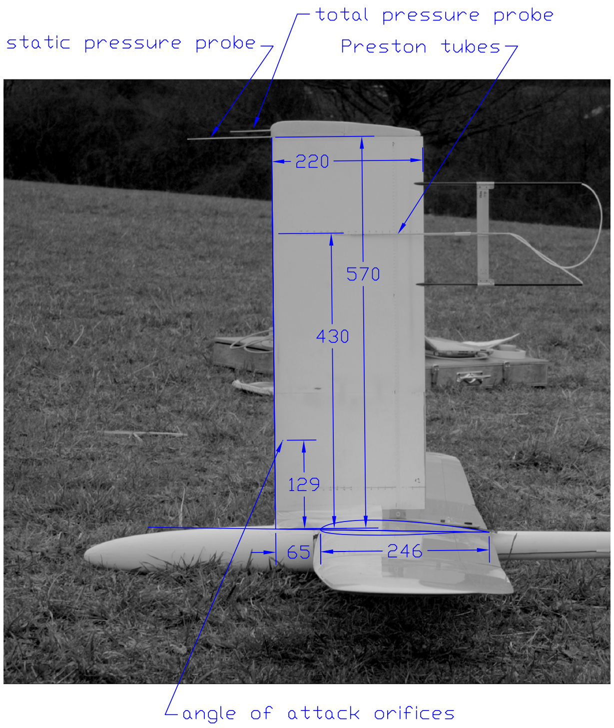

FIG. 4: Dimensions of the measurement airfoil and position towards fuselage and airfoil of the carrier plane

to a glider model plane shown in figure 5. Thus the angle of attack of 0° can be maintained at stationary speeds between 10 and 50 $\frac{m}{s}$. The eigenfrequency of the airplane of 1 to 2 Hz at 1 to 2° amplitude is adequately low due to a low moment of inertia and a high flight mechanical dynamic stability around the vertical axis. The periodic time is thus sufficiently long compared to the time for the flow around the measurement profile. So in spite of the oscillation a quasi-stationary state can be assumed at the profile. The measurement airfoil is attached to the carrier airplane above the t/4-line of its wing. The isobars of the pressure field around the airfoil of the carrier airplane run horizontally, thus it possesses a minimal impact on the TS amplification at the measurement airfoil. Comparing calculations of TS-wave amplification considering the pressure field of the airfoil of the carrier airplane show an error smaller than 1% of the amplification factor.

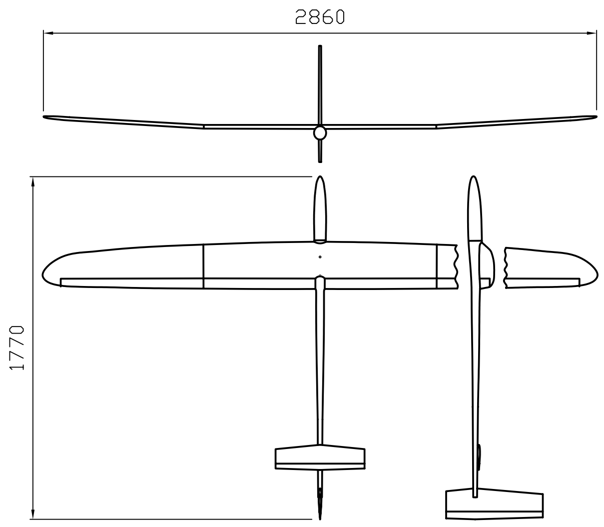

FIG. 5: The carrier plane

At the wing tip of the measurement airfoil a total pressure probe and a static pressure probe are attached to measure the flight velocity. At a distance of 100 mm from the lower end of the measurement airfoil at 5.5 % of the airfoil depth in the middle of the suction peak orifices of 0.3 mm diam are inserted symmetrically on both sides. Between these orifices the pressure difference is measured to determine the current angle of attack of the measurement airfoil.
Two Preston tubes are used to measure transition. They are attached 150 mm away from the wing tip and are placed exactly oppositely to control for symmetry. Thus they are outside the turbulence cone triggered by the wing tip and as far away as possible from the sphere of the airfoil of the carrier airplane. Preston tubes are total pressure probes, that are mounted to the profile surface and only measure the lower boundary layer area (figure 6). The laminar boundary layer shows slow velocities close to the wall and thus a very low total pressure, whereas the turbulent boundary layer shows a richer velocity profile for the same external pressure conditions. The pressure measures in the Preston tubes are hence greater for turbulent flow. The Preston tubes are retained to their position before each flight. Velocities are varied to move the laminar-turbulent transition area past the Preston tubes. To fully utilise the symmetry of the Preston tubes, the tube peaks were fitted to each other in the wind tunnel on a flat plate before the experiments.
Acceleration-compensated and temperature-stabilised pressure-difference sensors, type PCLA G1 from the

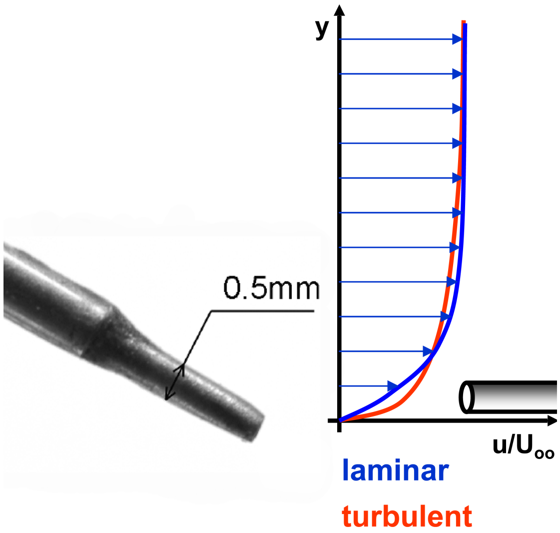

FIG. 6: Size and measurement principle of the Preston tubes

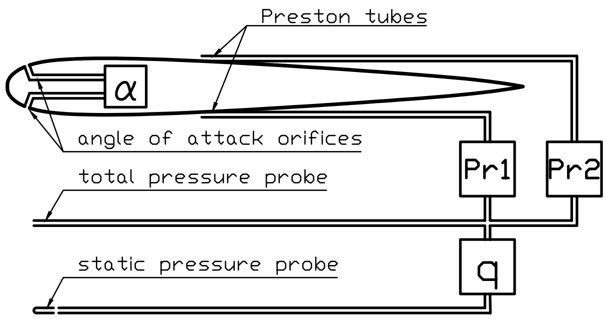

FIG. 7: Arrangement of the probes, pressure pipes and pressure-difference sensors

company Sensortechnics, are used for pressure measurement. The wiring of the used probes, pressure pipes and pressure-difference sensors is shown in figure 7. The signals coming from the pressure-difference sensors are amplified, low-pass filtered and recorded by a 10bit A/D converter. Data are recorded with a light telemetry device specially constructed for this research. They are transmitted in realtime to a PC on the ground. Thus the airplane can be controlled in accordance with the recordings of the sensors for velocity and angle of attack.
The measured pressures are corrected for remaining influences of the airfoils. To obtain thermophysical conditions temperature, air pressure and humidity are measured on the ground.
The measurement airfoil was also tested with the same sensor technology in the laminar wind tunnel of the "Institut für Aero- und Gasdynamik" at the "Universität Stuttgart" (Wortman and Althaus [19]) . The wind tunnel is of the Eiffel type and has got a closed measuring section as well as an open runback. The turbulence is homogeneous over the cross-section of the measurement chamber. The turbulence rate $Tu = \frac{\sqrt{u'}}{U_\infty}$ lies between 0.012 and 0.049 % for frequencies above 20 Hz, depending on the flow velocity. The measurement section has a height of 0.73 m, a width of 2.73 m and a depth of 3.15 m.

4 Determination of the transition position

The pressure coefficient for the Preston tubes is defined as

$$c_{p\,Preston} = \frac{p_{total} - p_{Preston}}{q_\infty}$$

To detect the transition position, all combinations for a fixed Preston tube position are plotted in a $c_{p\,Preston}$ - Re diagram (see figure 8). In the figure two constant areas with laminar and turbulent flow are displayed. The coefficients fall between these values, where the average velocity profile of the boundary layer transforms within the transition area. An interpolation function consisting of a sinus function and a tangential appended linear function is fitted to the measured values. Thus the starting transition can be determined even in case of dispersed measured values in that area.

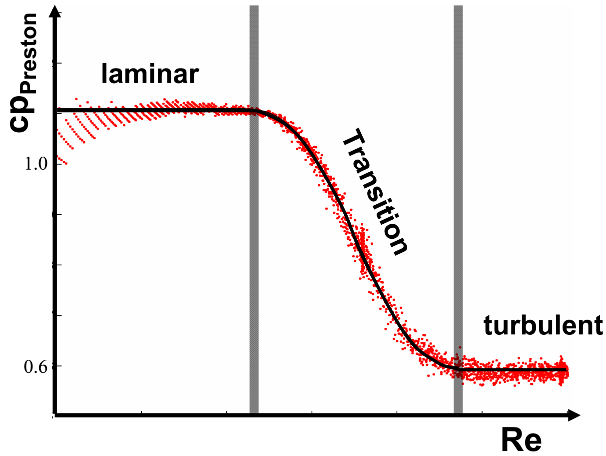

FIG. 8: Pressure coefficient of the Preston tube $c_{p\,Preston}$ against the free stream Reynolds number

To analyse the flight measurements the measured values are filtered according to the measured angle of attack and the symmetry of the Preston tubes. The analysed range of angles of attack can be narrowed up to 0.05° by means of the sensor. As the sensor could not be calibrated with this accuracy before the flights, the measured values are displayed in four colours in the $c_{p\,Preston} - Re$ diagram. It is distinguished, at which profile side the value is measured and from which direction the measured incoming flow comes. The sensor's "zero " position of angle of attack is adjusted such that the differences of the pressure coefficients of the Preston tubes at each side of the profile are minimised for every Reynolds number and that an equal number of measured values for incoming flow from the right and the left side can be displayed. The filter thresholds are narrowed until the diagram shows a clear trend.

5 Measurements

All flights took place near Stuttgart. The main measurement flights were done in calm air at sunrise with wind velocities below 0.1 $\frac{m}{s}$. The used airfield is in a wide plain area. For comparison, additional measurements were taken in moving air with wind velocities up to 3 $\frac{m}{s}$ and thermal lift in a hilly area for comparison. The free stream turbulence could not be measured and is therefore unknown.
In the wind tunnel-experiments the same equipment is used as in the flight tests. The Preston tubes are also fixed in several positions and the flight velocity is increased slowly. The transition position is additionally detected for several Reynolds numbers by stethoscope and an infrared thermal camera.

6 Results

6.1 Wind tunnel

The determined n-factors of the wind tunnel measurements are shown in figure 9. The series "Laminar wind tunnel IAG right " and "Laminar wind tunnel IAG left " display the n-factors, which are seperately determined from the measurements of each Preston tube.

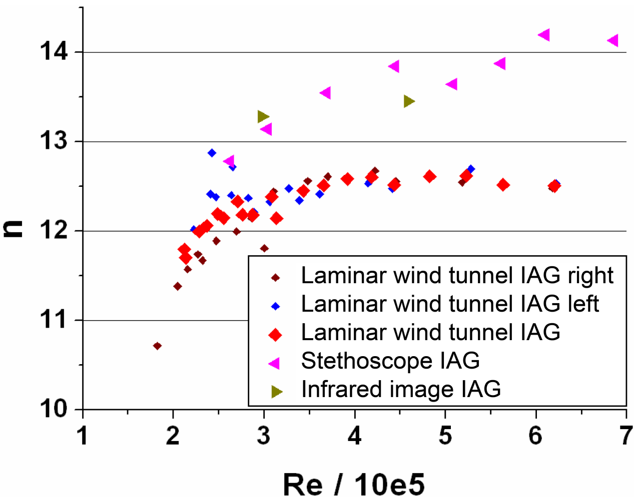

FIG. 9: N_{crit}-factors of the wind tunnel measurements

The position of the measurement profile was not changed during measurements, nevertheless a mainly small difference in transition position at the two profile sides could not be avoided. The series "Laminar wind tunnel IAG " was averaged from the results of both sides of the profile. The averaging is sufficiently exact if the difference in transition position is not too large. According to calculations in XFoil the transition positions move symmetrically for small angles of attack from the transition position, which is given at an angle of attack of $\alpha = 0°$. Moreover in that narrow range the TS amplitudes increase quasi-linearly with the profile depth.

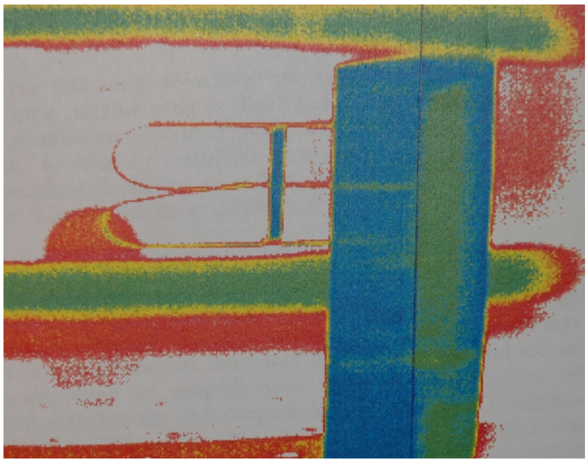

FIG. 10: Thermal image with $Re = 458,000$, incoming flow from the right side

The n_{crit} determined by use of the stethoscope and thermal images are higher as the n_{crit} determined in the measurements with Preston tubes. This is due to these methods: the turbulent interference velocities need to have a minimal size to be detectable by stethoscope and thermal images. Figure 10 displays a thermal image for $Re = 458\,000$. The start of transition is marked by a blue line. As the transition position is constant the flow arround the measurement airfoil is two-dimensional. At the wing tip a turbulence cone induced by the presure probes occurs. In the middle of the airfoil warm areas in direction of the flow can be seen. These are caused by heat storage in integrated rips and are of no importance to the flow around the airfoil.

6.2 Flight in calm air

The averaged results of the flights in calm air are presented in figure 11. The results from the wind tunnel tests are also shown for comparison.

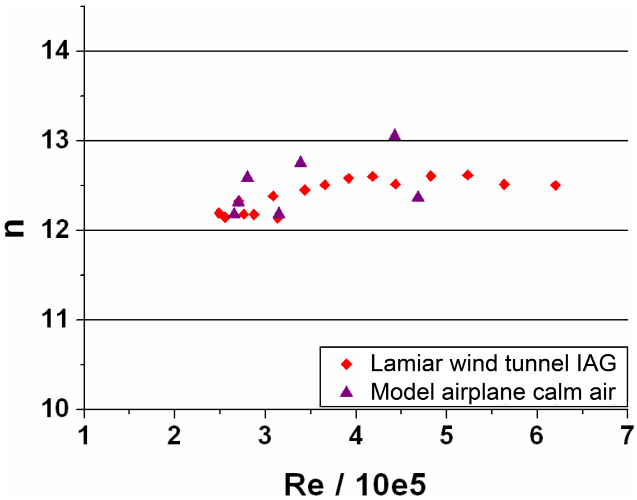

FIG. 11: N_{crit}-factors from flights in calm air and wind tunnel tests

6.3 Flight in moving air

Additional measurements were taken in moving air. As the freestream turbulence could not be measured, the results shall only be interpreted as a tendency how the critical amplification factors develop with increasing freestream turbulence. The averaged results of all flights are shown in figure 12.

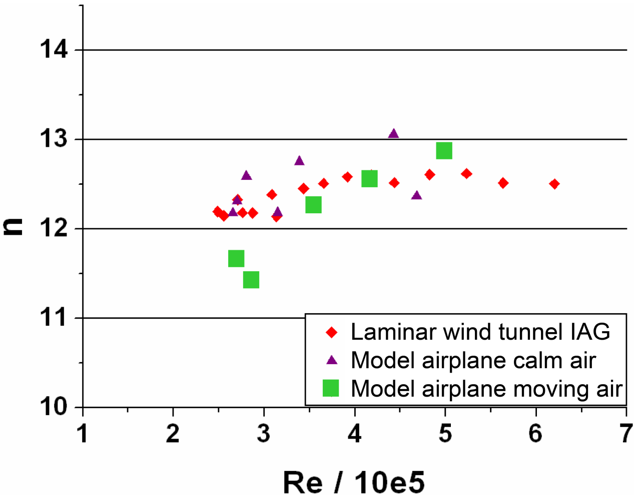

FIG. 12: N-factors from all flights and wind tunnel tests

6.4 TS-wave-frequencies and eddy-sizes

In figure 13 the frequency of the most amplified TS-wave, which is critical for transition, is plotted against the freestream Reynolds number and the amplification factor n. It can be expected that the more energy a frequency band of eddies contains, the more interference in the boundary layer is caused by these eddies.

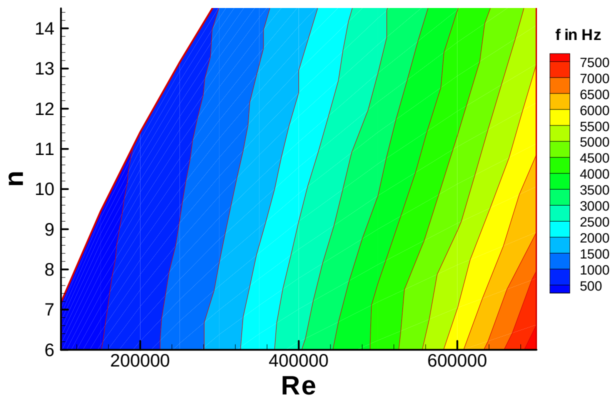

FIG. 13: Critical Tollmien-Schlichting-wave frequencies

According to the Tayler-hypothesis of frozen turbulence [9] the size of eddies in freestream can be calculated by means of the frequency with which they hit the airplane. The size of these eddies is displayed in figure 14.

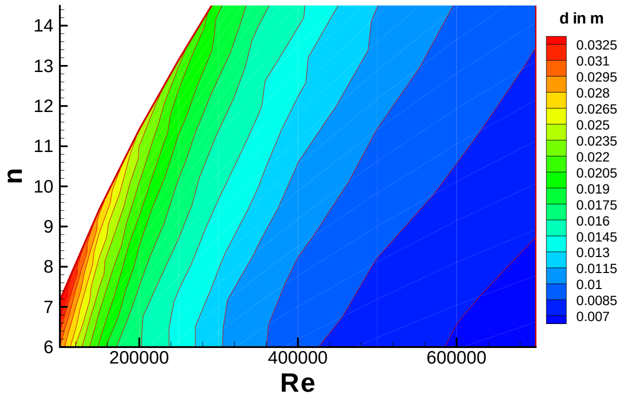

FIG. 14: Eddy sizes impinging on the measurement airfoil with critical TS-wave frequency

7 Discussion

Beyond $Re = 300,000$ the n_{crit} measured in free flight are between 12 and 13.2. They thus disperse symmetrically around the n-factors determined in the wind tunnel, which are $n_{crit} = 12.6 \pm 0.1$. According to Mack [16] the following empirically determined relationship exists between n_{crit} and the free stream turbulence level Tu:

$$n_{crit} = -8,43 - 2,4\ln(Tu)$$

The amplification factor $n_{crit} = 12.6$ thus corresponds to $Tu = 0.0156\,\%$. This is in agreement with the turbulence level stated by Würz [20] of the laminar wind tunnel: $0.012\,\% < Tu < 0.05\,\%$.
Beyond $Re = 300,000$ the n-factors do not change in moving air, i.e. the increased free stream turbulence does not appear to have an impact. This is contrary to Mack's equation. However it is in agreement with Bertolotti's finding, that a coupling into the boundary layer of the TS-waves is dependent on the specific characteristics of the frequency spectrum and the shape of the vortices in the free stream [1]. For a further interpretation an experimental determination of the exact shape of free stream turbulence seems necessary. It can not definitely be said that the moving air really has an higher amount of small scale turbulence, as it could not be measured. Never the less the found n-factors for $Re > 300,000$ in calm air can be regarded reliable due to the low dispersion and the concordance between measurements in the wind tunnel and free flight.
Below $Re = 300,000$ the measured n_{crit} decrease with decreasing Reynolds numbers. At the same time the difference in transition positions at both sides of the profile increases although the angle of attack is not changed. This effect ist due to assymetrical flow separation in the pressure rise at 90% of the profile depth that ocurs in low Reynolds numbers and very small angles of attack. As described in section 3 this effect can increase the lift gradient $\frac{\partial C_L}{\partial \alpha}$ up to 20π. The impact of this effect can be seen in the results of the wind tunnel measurements in figure 9. With decreasing Reynolds numbers the n_{crit} at the left side of the profile re-

main constant or even increase for very low Reynolds numbers, wheras the n-factors of the right side of the profile decrease as if the angle of attack would have been increased. In the flight measurements in moving air this decrease in n_{crit} ocures as well. In calm air the airplane does very small oscillations around its vertical axis. In moving air the measured oscillation amplitudes are much higher. As the zero crossing of C_L of the test airfol therefore is very fast with high lift gradient $\frac{\partial C_L}{\partial \alpha}$ in low Reynolds numbers, it is possible that the measuring equipment was too slow to record the $C_L = 0$ state reliably.

7.1 Comparison to other results

Lerch [13] did additional measurements on a Duo Discus T glider airplane with the same measurement airfoil developed here. The airplane with the measurement airfoil attached to it can be seen in figure 15. The results of these measurements are shown in figure 16. In Lerch's measurements the averaged amplification factor is $n_{crit} = 12.8$ with a small dispersion of ± 0.5.

FIG. 15: Measurement airplane Duo Discus T from Lerch [13]

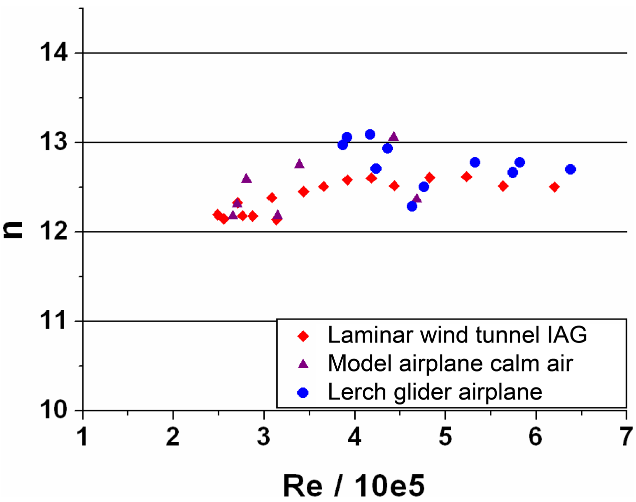

FIG. 16: Comparison to the n_{crit}-factors of Lerchs flights

Horstmann and Quast [8] determined n_{crit} for Reynolds numbers beyond 1,000,000. Flights were done in calm air above a thermal inversion layer to avoid thermal convection. Measurements were taken at a "glove" attached to the right airfoil. The glove's width is almost the profile depth. Measurements in the German Dutch wind tunnel (DNW) were done with the whole right airfoil in its closed measurement chamber. Transition positions are detected by means of an infrared camera. The TS-wave amplification is calculated with a direct, compressible Orr-Sommerfeld-solver.

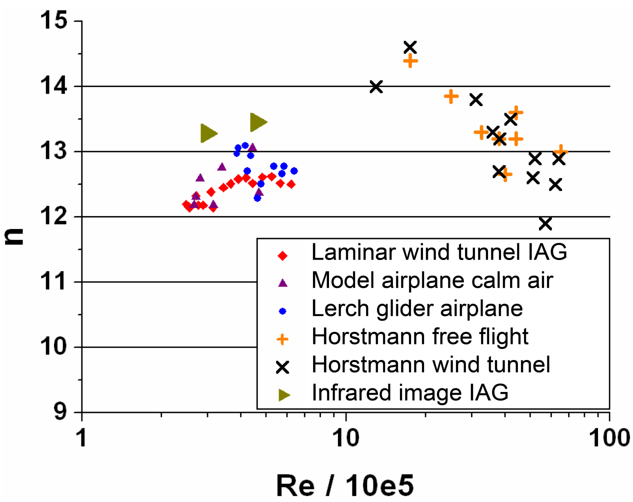

FIG. 17: Comparison to the n_{crit}-factors of Horstmanns measurements [8]

The resulting n-factors from Horstmann and Quast are between 12 and 15, thus they disperse around the value from the present research which was determined in the laminar wind tunnel using thermal images. They are slightly higher than the n-factors found here in free flight using Preston tubes. This is mainly due to the method defining the transition position, so the measured values are all in the same range. Small differences may result from different methods of stability analysis. Horstman and Quast did compressible calculations, here an incompressible solver was used.
Kroneberger [12] took measurements in free flight with a motor glider. The author found a critical amplification factor of $n_{crit} = 9$. This finding is considerably smaller than the results reported here. To analyse the TS-wave amplification Kroneberger used an indirect table solver assuming Falkner-Scan Profiles. The pressure distribution along the profile contour of the laminar glove, which is necessary for the calculations, is measured in a wind tunnel with an open measuring section. As the laminar glove has a width almost as the measuring section and shows a dilation <1, the measured pressure distribution may be affected by three-dimensional effects.

8 Conclusions

A new method could be developed to determine the critical amplification factors n_{crit} reliably and efficiently. The measurements show an averaged n_{crit}

of 12.6 for Reynolds numbers between 300,000 and 600,000. The obtained n_{crit}-factors have a very low dispersion of $\Delta n_{crit} = 0.1$ in the laminar wind tunnel and $\Delta n_{crit} = 0.6$ in free flight. No dependency on the free stream turbulence is observed. Below $Re = 300,000$ the dispersion of measured values increases considerably and the n-factors decrease. Further research is needed to clarify to what extent this result is caused by measurement errors.

References

[1] F. P. Bertolotti. *Effect of Atmospheric Turbulence on a Laminar Boundary-Layer.* CSTIV-99 XXVI Congress, Bayreuth.

[2] T. Cebeci and A. M. O. Smith. *Analysis of Turbulent Boundary Layer.* Academic, 1974.

[3] S. D. Conte. The Numerical Solution of Linear Boundary Value Problems. *SIAM Review*, 8(3), 1966.

[4] M. Drela and M. B. Giles. *Viscous-inviscid analysis of transonic and low Reynolds number Airfoils.* AIAA-86-1786-CP, 1986.

[5] G. Graf. Ermittlung des n-Faktors zur Umschlagbestimmung bei niedrigen Re-Zahlen. Student research project, Institut für Aero- und Gasdynamik, Universität Stuttgart, 1998.

[6] S. Herr. *Experimental Investigation of Airfoil Boundary-Layer Receptivity and a Method for the Characterization of the Relevant Free-Stream Disturbances.* PhD thesis, Institut für Aerodynamik und Gasdynamik, Universität Stuttgart, October 2003.

[7] K. H. Horstmann and S. J. Miley. Comparison of Flight and Wind Tunnel Investigations of Tollmien-Schlichting Waves on an Aircraft Wing. DGLR Proceedings, Hamburg, March 1992.

[8] K. H. Horstmann, A. Quast, and G. Redeker. Flight and Wind-Tunnel Investigations on Boundary-Layer Transition. *Journal of Aircraft*, 27(2):146–150, February 1990.

[9] J. C. Kaimal and J. J. Finnigan. *Atmospheric Boundary Layer Flows.* Oxford University Press, 200 Madison Avenue, New Yoek, 1 edition, 1994.

[10] B. Kobiela. Untersuchungen zum Grenzschichtumschlag bei kleinen Reynoldszahlen. Freiflug- und Windkanalexperiment. Diploma thesis, Institut für Aerodynamik und Gasdynamik, Universität Stuttgart, June 2006.

[11] B. Kobiela, A. Lerch, A. Herrig, and W. Würz, editors. *Grenz-N-Faktor Bestimmung bei Reynoldszahlen < 600 000. Ein neuer Ansatz für kombinierte Freiflug- und Windkanalmessungen.* Institut für Strömungsmechanik der TU Braunschweig, Symposium für Segelflugzeugentwicklung, September 2006.

[12] M. Kroneberger. *Multisensor-Heißfilmtechnik zur Transitionserkennung im Windkanal- und Flugversuch.* PhD thesis, Technische Hochschule Aachen, 1992.

[13] A. Lerch. Untersuchungen zum Grensschichtumschlag bei minimaler Anströmturbulenz. Student research project, Institut für Aerodynamik und Gasdynamik, Universität Stuttgart, 2006.

[14] Th. Lutz, W. Würz, and S. Wagner. Numerical Optimization and Wind-Tunnel Testing of Low Reynolds-Number Airfoils. *Thomas J. Mueller (ed.): Fixed and Flapping Wing Aerodynamics for Micro Air Vehicle Applications*, 195, AIAA 2001.

[15] L. M. Mack. Boundary-Layer Linear Stability Theory. *AGARD Report, Special Course on Stability and Transition of Laminar Flow*, (709):3 – 8.

[16] L. M. Mack. Transition Prediction and Linear Stability Theory. *AGARD Conf. Proc.*, (224):1–22, 1977.

[17] S. J. Miley and K. H. Horstmann. Data Report of Flight and Wind-Tunnel Investigations of Tollmien-Schlichting Waves on an Aircraft Wing. Technical report, Deutsche Forschungsanstalt für Luft- und Raumfahrt e.V., Braunschweig.

[18] W. S. Saric. Laminar-Turbulent-Trasition: Fundamentals. *AGARD Report 786: Special Course on Skin Friction Drag Reduction*, 1992.

[19] F. X. Wortman and D. Althaus. Der Laminarwindkanal des Instituts für Aerodynamik und Gasdynamik der Technischen Hochschule Stuttgart. *Zeitschrift für Flugwissenschaften*, 4(12), 1964.

[20] W. Würz. *Hitzdrahtmessungen zum laminar-turbulenten Strömungsumschlag in anliegenden Grenzschichten und Ablöseblasen sowie Vergleich mit der linearen Stabilitätstheorie und empirischen Umschlagskriterien.* PhD thesis, Institut für Aero- und Gasdynamik, Universität Stuttgart, 1997.